PROCEEDINGS OF SPIE

SPIEDigitalLibrary.org/conference-proceedings-of-spie

Improvement on impedance model of electromagnetic energy harvesting systems

Hong Tang, Yiming Gao, Junrui Liang

Hong Tang, Yiming Gao, Junrui Liang, "Improvement on impedance model of electromagnetic energy harvesting systems," Proc. SPIE 10967, Active and Passive Smart Structures and Integrated Systems XII, 1096726 (21 March 2019); doi: 10.1117/12.2515304

SPIE.

Event: SPIE Smart Structures + Nondestructive Evaluation, 2019, Denver, Colorado, United States

Improvement on impedance model of electromagnetic energy harvesting systems

Hong Tang, Yiming Gao, and Junrui Liang

School of Information Science and Technology, ShanghaiTech University
No. 393, Middle Huaxia Road, Pudong, Shanghai 201210, China

ABSTRACT

The existing equivalent impedance model of electromagnetic energy harvesters (EMEH) has considered only the single-harmonic relations among the current, voltage, velocity, and force in the dynamic electromechanical system. The modeling accuracy is insufficient, given the interference of high-order harmonics, which gets more severe under practical low-Q (quality factor) induction coil designs. This paper introduces an improvement to the conventional single-harmonic model by taking into account the influence of the practical low-Q coil and the high-order harmonics in the EMEH system. The extended impedance method (EIM) is used to characterize the nonlinear components in the system. The modeling accuracy by using EIM is improved. The theoretical result better matches the experimental one.

Keywords: Electromagnetic, energy harvesting, impedance analysis, extended impedacne method

1. INTRODUCTION

The energy harvesting technologies are extensively investigated as a promising and everlasting power supply solution for the IoT (Internet of Thing) devices.[1–4] Among these technologies, the kinetic energy harvesting technology scavenges the mechanical energy associated with mechanical motions and vibrations. When equipped with the kinetic energy harvesting unit, future distributed and wearable electronics might become self-powered when they are exposed to specific mechanical movements. Electromechanical transducers play a crucial role in the kinetic energy harvesting systems. The electromagnetic (EM) transducer is one of the most investigated transducers utilized for kinetic energy harvesting.

The electromagnetic energy harvester (EMEH) operates according to the Faraday's law of induction. Therefore, mechanical reciprocating movement induces alternating electrical voltage across the electrical port of an EM transducer. On the other hand, digital electronics use dc power for logic computing; the generated energy from the EMEH cannot be directly used to power the electronics. An ac-to-dc power conditioning circuit is necessary for the practical implementations. Different power conditioning circuits have been developed for dealing with the electrical output from the EM transducers. Generally speaking, the EM transducers give relative large current but low voltage electrical output; therefore, in many designs, the voltage boosting technologies are used in the ac stage, e.g., using a voltage multiplier,[4] or the dc stage, e.g., using a boost converter after the ac-to-dc rectification.[1,2]

Besides the circuit design, the understanding on the electromechanical joint dynamics is another crucial issue for evaluating the backward coupling effect of the nonlinear power conditioning circuit on the mechanical source. Such insight facilitates the collaborative electromechanical design and optimization. Some models have been proposed for analyzing the dynamics and predicting the harvested power of the EMEH systems.[5–7] In many analyses taking sides in the mechanical dynamics, the dynamics of the power conditioning circuit was equivalently regarded as an unconstrained passive electrical load,[6] which turned out to be insufficient for emulating the actual dynamics of a nonlinear power conditioning circuit. Cheng et al.[5] have considered the dynamics of a half-wave rectifier circuit through circuit simulation software tool, i.e., numerical simulation. Liang et al. have proposed an more intuitive and uniform impedance model for understanding the EMEH dynamics when it is connected to a full-wave bridge rectifier.[7] In essence, such impedance model is a single-harmonic approximation for the EMEH

Corresponding author: Junrui Liang. E-mail: liangjr@shanghaitech.edu.cn.

Active and Passive Smart Structures and Integrated Systems XII, edited by Alper Erturk, Proc. of SPIE
Vol. 10967, 1096726 · © 2019 SPIE · CCC code: 0277-786X/19/$18 · doi: 10.1117/12.2515304

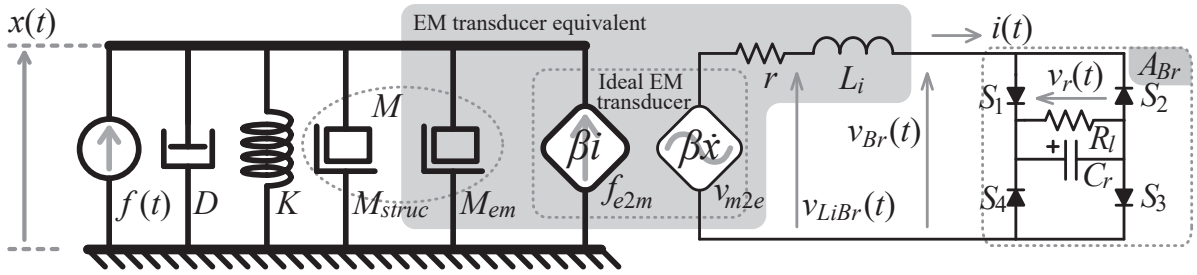

Figure 1. Schematic of an EMEH system using full-wave bridge rectifier.

systems, since it was established based on the single-harmonic current/voltage assumption. In the following parts of this paper, such impedance modeling method is referred to as the conventional impedance model (CIM).

By assuming the sinusoidal voltage across the coil inductance and harvesting circuit combination (the parasitic resistance r is singled out for later consideration), the CIM can roughly predict the level and changing trend of the experimental harvested power,[7] except the mismatch under some loading conditions. The reason of mismatching comes from the single-harmonic assumption at the very beginning, from which the waveform equations were derived. Such assumption can be only achieved by using a practically unreachable high-Q (quality factor) coil, i.e., the equivalent series resistance (ESR) r must be much smaller than the inductive reactance ωL_i in a physical coil. This paper aims to carry out a better evaluation for revealing such modeling mismatching and provide a multi-harmonics compatible extended impedance method (EIM) for improving the modeling accuracy of the EMEH systems.

2. EMEH SYSTEM

The schematic of an EMEH system is shown in Figure 1. It is composed of three parts: the *mechanical structure*, the *EM transducer* and the *power conditioning circuit*. The mechanical structure delivers the kinetic energy to the EM transducer. A part of the input mechanical energy is then transformed into electrical form. Finally, the interface circuit rectifies the ac power into dc form. The full-wave bridge rectifier is the most ready-to-use circuit for carrying out the ac-to-dc conversion.

The EM transducer is the key component of an EMEH system. The mutual electromechanical transduction is based on the Lorentz force law and Faraday's law of induction. An ideal linear EM transduction can be characterized with the following set of coupling equations

$$\begin{cases} f_{e2m}(t) = \beta i(t), \\ v_{m2e}(t) = \beta \dot{x}(t), \end{cases} \tag{1}$$

where β is the electromechanical coupling factor; $i(t)$ is the current on the electrical side; $f_{e2m}(t)$ represents the electrical-to-mechanical induced Lorentz force; $x(t)$ denotes the vibration displacement, whose derivative $\dot{x}(t)$ is the velocity; $v_{m2e}(t)$ is the mechanical-to-electrical induced electromotive force (voltage). A practical EM transducer includes some parasitic physical features, as shown in the gray area of Figure 1: M_{em} denotes the inherent mass of the mechanical moving part of a EM transducer, while L_i and r are the inherent inductance and ESR of the coil of an EM transducer, respectively. When connected to the mechanical vibrator, M_{struc}, D, and K, the structural mass, damping, and stiffness are added on the mechanical side to form the resonant dynamics. $f(t)$ in Figure 1 is the equivalent force exerted by the mechanical vibration source. For the electrical side, the external power conditioning circuit considered in this study includes: four diodes S_1, S_2, S_3, and S_4, which forms a full-wave bridge rectifier; C_r as the filter capacitor; and R_l as the equivalent dc load resistor. The bridge rectifier is a nonlinear component, since a linear system cannot generate dc output from an ac input. How to properly and uniformly express the dynamics of the nonlinear circuit and the linear vibrator is the key problem of the electromechanical joint modeling of EMEH. Liang et al.[7] have made a linear (single harmonic) approximation by taking the dynamics of the combination of bridge rectifier, C_r and R_l as an equivalent linear operator A_{Br}, as shown in Figure 1, such that the current through and voltage across A_{Br}, i.e., $i(t)$ and $v_{Br}(t)$, respectively, are

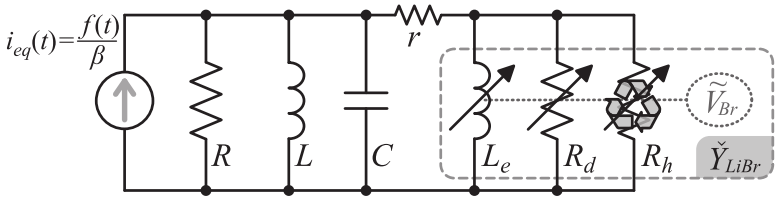

Figure 2. Equivalent impedance network model of an EMEH system using full-wave bridge rectifier under the CIM single-harmonic approximation.

equivalently regarded as pure sinusoidal waves. With the concept of A_{Br} operator, the constitutive equations for the EMEH system are formulated as follows

$$\begin{cases} f(t) = M\ddot{x}(t) + D\dot{x}(t) + Kx(t) + \beta i(t), \\ \beta\dot{x}(t) = ri(t) + L_i\dot{i}(t) + A_{Br}[i(t)]. \end{cases} \tag{2}$$

The schematic shown in Figure 1 includes mechanical and electrical components, whose dynamic is no easy to articulate in an uniform way. The usual solution is to convert the dynamic relation on one domain to their equivalents on the other domain by taking the electromechanical analogy. For example, as shown in Figure 2, the linear mechanical components can be modeled by their electrical equivalents by taking the electromechanical analogy as follows

$$i_{eq}(t) = \frac{f(t)}{\beta}; \qquad C = \frac{M}{\beta^2}; \qquad R = \frac{\beta^2}{D}; \qquad L = \frac{\beta^2}{K}. \tag{3}$$

In the electromechanical analogy, the force source is equivalent to a current source; the mass, damping, and stiffness in the mechanical domain are equivalent to capacitance, resistance, and inductance, respectively.

3. CONVENTIONAL IMPEDANCE MODEL AND ITS LIMITATION

Given a mechanical vibrator operates around one of its resonant frequencies, the mechanical structure acts as a filter. Therefore, no matter what power conditioning circuit is connected, the vibration motion $x(t)$ and its derivative velocity $\dot{x}(t)$ are very close to a single harmonic, i.e., sinusoidal wave. Since the mechanical-to-electrical induced voltage source $v_{m2e}(t)$ is proportional to the velocity, it can be regarded as pure harmonic voltage too.

The term impedance in the conventional ac circuit analysis describes the magnitude and phase relations between two harmonic "across variable" and "through variable", which is a concept characterizing the linear dynamics of a component or a component network.

In the CIM,[7] the analysis starts from the assumption of harmonic voltage across the L_i and bridge rectifier combination network, i.e.,

$$v_{LiBr}(t) = V_{LiBr}\sin(\omega t), \tag{4}$$

where ω is the vibration frequency, V_{LiBr} is the magnitude. The current flowing through L_i, i.e., $i(t)$ in Figure 1 is able to be formulated based on the piecewise integral of the voltage across the inductance L_i, i.e., $v_{Li}(t) = v_{LiBr}(t) - v_{Br}(t)$. The piecewise current expression is shown as follows

$$i(t) = \frac{V_{LiBr}}{\omega L_i} \times \begin{cases} -\cos\theta - \tilde{V}_{Br}\theta\Big|_{\theta=2k\pi+\theta_0}^{\omega t}, & 2k\pi+\theta_0 \le \omega t < 2k\pi+\theta_1; \\ 0, & 2k\pi+\theta_1 \le \omega t < 2k\pi+\pi+\theta_0; \\ -\cos\theta + \tilde{V}_{Br}\theta\Big|_{\theta=2k\pi+\theta_0}^{\omega t}, & 2k\pi+\pi+\theta_0 \le \omega t < 2k\pi+\pi+\theta_1; \\ 0, & 2k\pi+\pi+\theta_1 \le \omega t < 2k\pi+2\pi+\theta_0; \end{cases} \tag{5}$$

where $\tilde{V}_{Br}$ is the normalized expression of V_{Br}, which is formulated as follows

$$\tilde{V}_{Br} = \frac{V_{Br}}{V_{LiBr}} = \frac{V_r + V_F}{V_{LiBr}}. \tag{6}$$

V_F is the forward voltage drop of the rectifier and V_r is the dc voltage across C_r. In (5), the two angle θ_1 and θ_0 should be determined according to the current conduction modes of the inductor L_i. More information about the operation of the two continuous and discontinuous conduction modes (CCM and DCM) can be found in the original paper introducing CIM.[7]

Since the impedance concept describing the relation between two sinusoids under at the same frequency, the equivalent impedance of the L_i and bridge rectifier combination cannot be derived with the expressions on $v_{LiBr}(t)$ and $i(t)$, i.e., (4) and (5). The key technique here is not to compare $v_{LiBr}(t)$ and $i(t)$, but $v_{LiBr}(t)$ and $i_F(t)$, the fundamental harmonic of $i(t)$, which can be obtained by using the numerical method according to the admittance formula in the frequency domain as follows

$$\check{Y}_{LiBr}(j\omega) = \frac{I_F(j\omega)}{V_{LiBr}(j\omega)}. \tag{7}$$

It turns out that admittance, the inverse of impedance, is more convenient than impedance in the calculation for EMEH. To separately specify the different dynamic effects of the admittance $\check{Y}_{LiBr}(j\omega)$, it was further divided into three components as follows

$$\check{Y}_{LiBr}(j\omega) = G_h + G_d + jB_e = \frac{1}{R_h} + \frac{1}{R_d} + \frac{1}{j\omega L_e}, \tag{8}$$

where G_h and G_d are the harvested component and dissipated component, respectively, characterizing the energy harvesting and energy dissipation, whose combination has a mechanical damping effect; B_e is the inductive subseptance, which is result from the inductive feature of the EM transducer. The values of the three effective dynamic components are functions of the rectified voltage $\tilde{V}_{Br}$, as illustrated in Figure 2. Equations (4) to (8) formulate the key steps of the linear approximation of the EMEH system, which leads to the equivalent impedance network model of the whole system, as shown in Figure 2. With this equivalent impedance model, the voltages, current, and power of each component can be readily calculated based on the established circuit laws.

The CIM provides a reasonable prediction on the harvested power, as it shows similar level and changing trend, compared to the experimental result.[7] Yet, the theoretical result with CIM still has some mismatching to the experimental points under specific loading condition. Model improvement is needed towards better description on the joint dynamics.

Through parametric studies with circuit simulation tool, we find that the problem comes from the limited quality factor Q in practice, which undermines the sinusoidal $v_{LiBr}(t)$ assumption at the beginning of the CIM derivation. Figure 3 shows the current and voltage waveforms under different Q values. $v_{m2e}(t)$ is pure sinusoidal as it is proportional to the vibration velocity, whose high-order harmonics are filtered by the mechanical vibrator. Since $v_{m2e}(t) = v_{ESR}(t) + v_{LiBr}(t)$, sinusoidal $v_{LiBr}(t)$ is valid only under zero or very small $v_{ESR}(t)$, i.e., r is much smaller than the reactance ωLi, or in other words, large Q value, since $Q = \omega Li/r$. As we can observe from Figure 3(f), the sinusoidal $v_{LiBr}(t)$ assumption can be hardly accepted when $Q < 1$. But for practical air coil under low-frequency mechanical vibration excitation, Q is not easy to attain a high value. Therefore, general speaking, increasing L_i and decreasing the ESR can improve the accuracy of CIM, i.e., the CIM performs better under high-Q condition.

4. EXTENDED IMPEDANCE MODEL

To overcome the limitation of CIM method, which can only consider the fundamental harmonic, we introduce a new modeling technique called the EIM method for analyzing the EMEH system. The principle of EIM is briefed in the Appendix A. It is a multiple harmonic based iterative method for formulating the steady state of nonlinear circuits. Since there is not such sinusoidal $V_{LiBr}(t)$ requirement for EIM formulation, it can take into account the small Q condition.

The flow charts of CIM and EIM are summarized in Figure 4. At the beginning, the circuit should have the initial states (voltage/current) by assuming that the diodes are all conducted. Then, the initial states of the

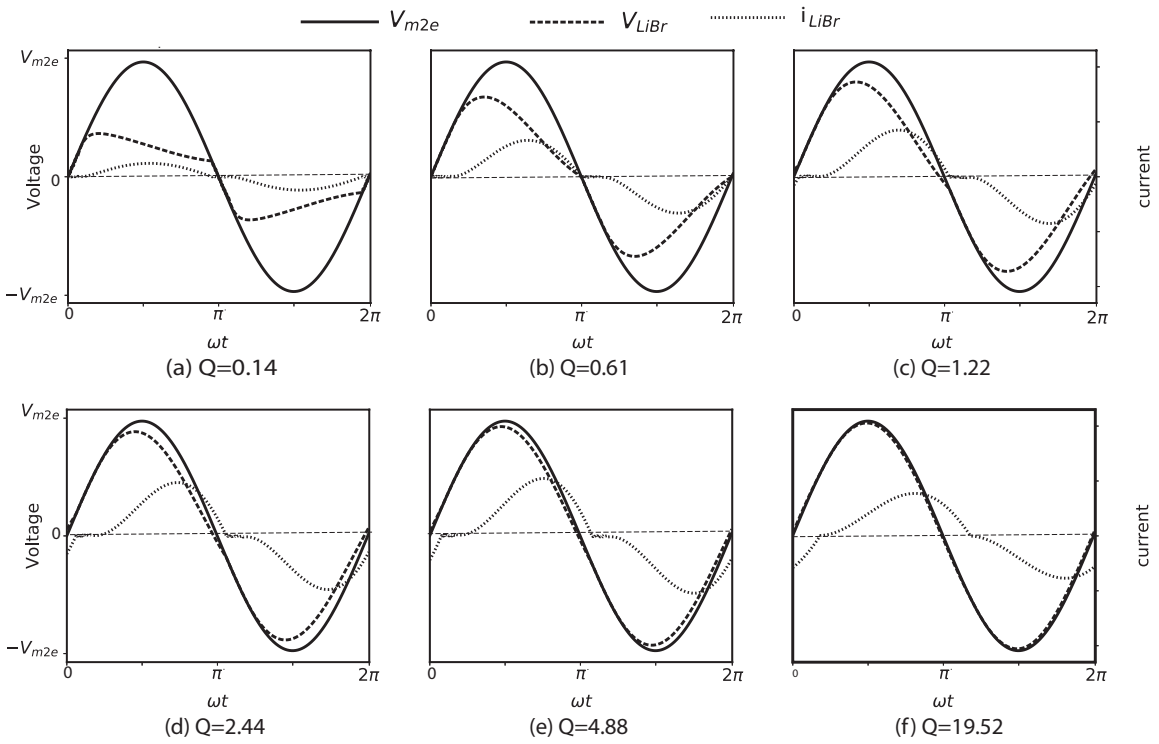

Figure 3. Waveforms of V_{m2e}, V_{LiBr}, and i_{LiBr} under different Q (quality factor) values.

circuit can be obtained (block 1). The key steps include state-to-time mapping (block 2) and formulating the extended impedance matrix (block 5). As the operation states (voltages or currents) are unknown before the circuit runs, a relative tolerance needs to be set for the iterative formulation.[8]

In the view of EIM, a diode can be represented by a state-dependent resistor. The EMEH impedance network can be specified much easier as that shown in Figure 5. The components R_{D1}, R_{D2}, R_{D3}, and R_{D4} represent four state-dependent resistors, whose resistance changes according to their terminal voltages. The constitutive relation of this circuit network can be formulated as follows by applying the nodal analysis.

$$\begin{bmatrix} \mathbf{V}_{\mathbf{m2e}}^{(n+1)} \\ \mathbf{V}_{\mathbf{Br}}^{(n+1)} \\ \mathbf{V}_{\mathbf{1}}^{(n+1)} \\ \mathbf{V}_{\mathbf{2}}^{(n+1)} \end{bmatrix} = \begin{bmatrix} \mathbf{Y_{RLC}} + \mathbf{Y_{Li}} & -\mathbf{Y_{Li}} & \mathbf{0} & \mathbf{0} \\ \mathbf{Y_{Li}} & -\left(\mathbf{Y_{Li}} + \mathbf{Y}_{\mathbf{D1}}^{(n)}\right) & \mathbf{Y}_{\mathbf{D1}}^{(n)} & \mathbf{Y}_{\mathbf{D2}}^{(n)} \\ \mathbf{0} & \mathbf{Y}_{\mathbf{D1}}^{(n)} & -\left(\mathbf{Y}_{\mathbf{D1}}^{(n)} + \mathbf{Y}_{\mathbf{D3}}^{(n)} + \mathbf{Y_{load}}\right) & \mathbf{Y_{load}} \\ \mathbf{0} & \mathbf{Y}_{\mathbf{D2}}^{(n)} & \mathbf{Y_{load}} & -(\mathbf{Y}_{\mathbf{D2}}^{(n)} + \mathbf{Y}_{\mathbf{D4}}^{(n)} + \mathbf{Y_{RLC}}) \end{bmatrix}^{-1} \begin{bmatrix} \mathbf{I_{eq}} \\ \mathbf{0} \\ \mathbf{0} \\ \mathbf{0} \end{bmatrix}, \tag{9}$$

where $\mathbf{Y_{RLC}}$ is the total admittance of R, L, and C; $\mathbf{Y_{Li}}$ is the admittance of L_i and r; $\mathbf{Y_{load}}$ is the admittance of the parallel R_l and C_r; and $\mathbf{Y_{D1}}$, $\mathbf{Y_{D2}}$, $\mathbf{Y_{D3}}$, $\mathbf{Y_{D4}}$ are the admittance of four diodes, respectively. The superscripts (n) and $(n+1)$ indicate the number of iteration. The four diodes are initially assumed conducting in the first iteration. The obtained result will be submitted to the next round of calculation and so forth until the examined voltage V_{D1}, which is terminal voltage of D_1, meets its relative tolerance.

The output voltage of the circuit V_{rect} is $V_1 - V_2$. Therefore, the theoretical harvested power is formulated

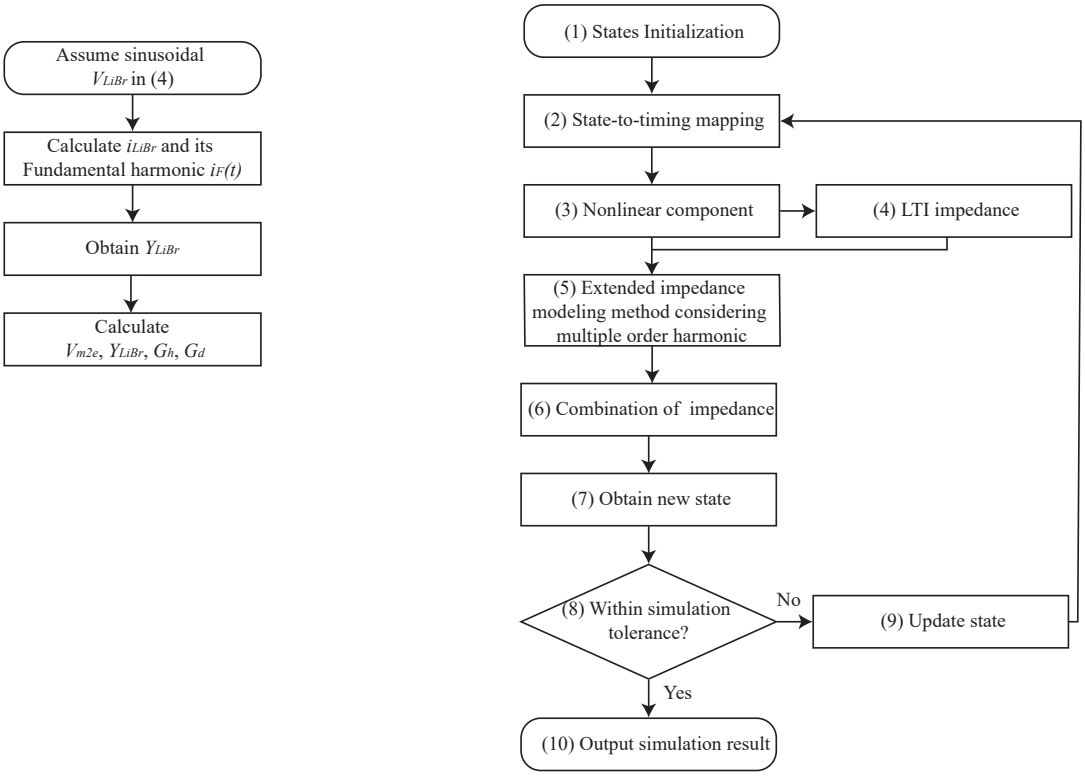

(a) CIM (b) EIM

Figure 4. Flow charts for conventional single-harmonic based impedance modeling (CIM) and the multiple-harmonics based extended impedance method (EIM).

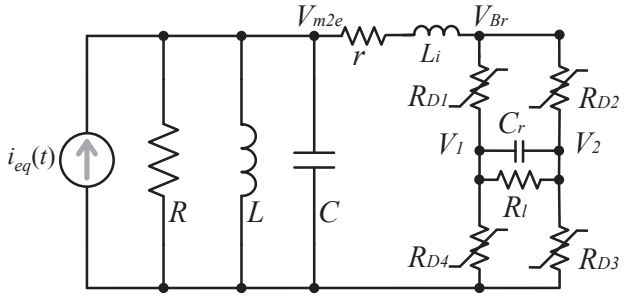

Figure 5. The equivalent extended-impedance network of an EMEH system using full-wave bridge rectifier.

as follows

$$P_h = (\mathbf{V_1} - \mathbf{V_2})^T \mathbf{Y_{load}} (\mathbf{V_1} - \mathbf{V_2}) \tag{10}$$

5. EXPERIMENTS

Experiment is carried out to validate the EIM analysis and its improvement compared to CIM. The experimental parameters, which are listed in Table 5 are from the existing CIM paper.[7] Those parameters include identified dynamic parameters and experiment conditions. The identified parameters describe the equivalent internal dynamics of the mechanical structure and EM transducer. The internal impedance is specified as $\check{Z}_{in}$ in (11). The detailed component values in $\check{Z}_{in}$ can be obtained by fitting the impedance measurement results from an

Table 1. Parameter values and experimental conditions.[7]

Parameter	Value	Experiment conditions	Value
R	216 Ω	Base acceleration $\ddot{Y}$	1.5 g
L	4.042 mH	V_{oc} under $\ddot{Y}$	6 V
C	0.32 mF	Operating frequency f	139 Hz
L_i	272.62 mH	Rectifier voltage drop V_F	0.47 V
r	839.20 Ω		
β	1.70 N/A		
Q	0.284		

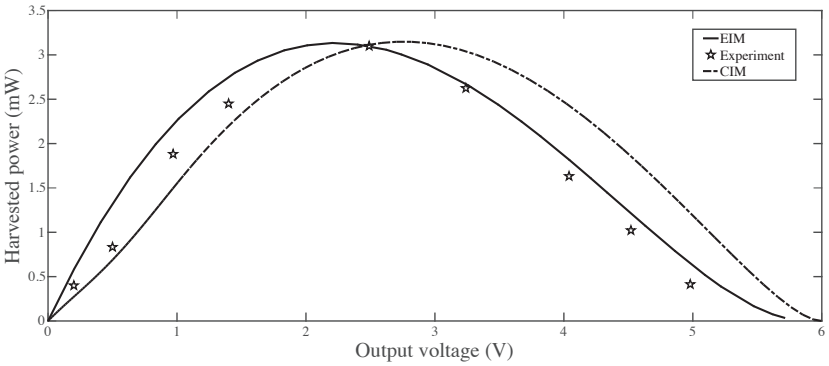

Figure 6. The result of harvested power.

impedance analyzer.

$$\check{Z}_{in}(j\omega) = r + j\omega L_i + \left(R \parallel j\omega L \parallel \frac{1}{j\omega C}\right) \tag{11}$$

The experiment device is composed of a vibration framework, a cantilever beam whose free end has two two magnets, as a part of the transducer, an induction coil fixed on the framework, and the power conditioning circuit. The framework vibrates around the resonant frequency of the beam. The relative movement between the magnet and coil has introduced a changing magnetic field in the coil, such that an electromotive force is induced through the electromagnetic induction.

The theoretical results obtained with CIM (dashed), EIM (solid), and experiment (star markers) are comparatively shown in Figure 6. It shows that the EIM result can better approach the experimental data points than the CIM one. For better quantify the improvement, an error function is introduced in (12) for evaluating the theoretical prediction of different methods, i.e.,

$$J = \frac{1}{N}\sum_{i=1}^{N}\frac{|P_T(V_{Ei}) - P_{Ei}|}{P_{Ei}}, (1 \le i \le N) \tag{12}$$

P_{Ei} denotes the ith experimental harvested power and V_{Ei} the ith experimental output voltage. The $P_T(v)$ is the expression of theoritical harvested power of the CIM or EIM, by fitting the corresponding data. N denotes the number of the experimental result. Define that J_{EIM} and J_{EIM} are the errors for EIM and CIM, respectively. J_{EIM} is 0.1961 and J_{CIM} is 0.3196, which proves that the EIM method is more accurate.

6. CONCLUSION

The electromagnetic energy harvesting (EMEH) system with a power conditioning circuit was not accurately modeled, because of the introduction of the nonlinear components. This paper introduces the extended impedance method (EIM) for the analysis. The EIM analysis has made some improvements towards better modeling

accuracy, compared with existing conventional impedance method. It also simplifies the simulation of EMEH system with a full-bridge rectifier, whose dynamics cannot be easily solved by basic circuit laws.

APPENDIX A. EXTENDED IMPEDANCE METHOD (EIM)

A.1 State-dependent resistance

Circuit components can be classified as two large sorts, linear ones, such as resistor, inductor, and capacitor, and nonlinear ones, such as diode and transistor. For the nonlinear components, the constitutive relation between voltage and current changes when its state (voltage/current) changes. For example, the conduction of a diode changes as its terminal voltage changes. From the viewpoint of EIM,[9,10] the diode can be modeled as a state-dependent resistor, whose value can be formulated as follows

$$r_d[v(t)] = \begin{cases} \infty, & v(t) \le 0; \\ \dfrac{v(t)}{I_S[e^{-v(t)/(nV_T)} - 1]}, & v(t) > 0, \end{cases} \tag{13}$$

where I_S is the saturation current of the diode; v_d is the forward voltage drop of the diode; V_T is the thermal voltage; n is the ideal factor.

A.2 Impedance in matrix form

In (13), r_d expresses the relation in time domain. Since $v(t)$ is a function of time, we can map the $r_d(v)$ under specific voltage v as function of time, i.e., $r_d(t)$, such that we have

$$v(t) = r_d(t)i(t), \tag{14}$$

The multiplication relation in (14) can be converted into convolution in the frequency domain as follows

$$V(j\omega) = R_d(j\omega) * I(j\omega), \tag{15}$$

where the $V(j\omega)$, $R_d(j\omega)$ and $I(j\omega)$ are the Fourier transform of $v(t)$, $r_d(t)$ and $i(t)$, respectively.

For periodic voltage, current, and resistance, their Fourier transform can be expressed with the discrete infinite impulses at the multiples of the fundamental harmonic frequency. The convolution in (15) therefore can be expressed in the discrete form, i.e.,

$$V_k = \sum_{n=-\infty}^{\infty} R_{k-n} I_n, \tag{16}$$

or in the vector and matrix form

$$\begin{bmatrix} \vdots \\ V_{-k} \\ \vdots \\ V_0 \\ \vdots \\ V_k \\ \vdots \end{bmatrix} = \begin{bmatrix} \ddots & \ddots & \ddots & \ddots & \ddots & \ddots & \ddots \\ \ddots & R_{d,0} & \ddots & R_{d,-k} & \ddots & R_{d,-2k} & \ddots \\ \ddots & \ddots & \ddots & \ddots & \ddots & \ddots & \ddots \\ \ddots & R_{d,k} & \ddots & R_{d,0} & \ddots & R_{d,-k} & \ddots \\ \ddots & \ddots & \ddots & \ddots & \ddots & \ddots & \ddots \\ \ddots & R_{d,2k} & \ddots & R_{d,k} & \ddots & R_{d,0} & \ddots \\ \ddots & \ddots & \ddots & \ddots & \ddots & \ddots & \ddots \end{bmatrix} = \begin{bmatrix} \vdots \\ I_{-k} \\ \vdots \\ I_0 \\ \vdots \\ I_k \\ \vdots \end{bmatrix}. \tag{17}$$

By further assuming that the harmonics whose orders are higher than K can be neglected. The periodic voltage $v(t)$ and current $i(t)$ can be represented in vectors composed of truncated Fourier series as follows

$$\mathbf{V} = [V_{-K} \quad \cdots \quad V_{-1} \quad V_0 \quad V_1 \quad \cdots \quad V_K]^T, \tag{18}$$

$$\mathbf{I} = [I_{-K} \quad \cdots \quad I_{-1} \quad I_0 \quad I_1 \quad \cdots \quad I_K]^T. \tag{19}$$

The truncated approximation of (15) can be obtained as follows

$$\mathbf{V} = \mathbf{R_d}\mathbf{I}, \tag{20}$$

where

$$\mathbf{R_d} = \begin{bmatrix} R_{d,0} & \dots & R_{d,-k} & \dots & R_{d,-2k} \\ \vdots & \ddots & \ddots & \ddots & \vdots \\ R_{d,k} & \ddots & R_{d,0} & \ddots & R_{d,-k} \\ \vdots & \ddots & \ddots & \ddots & \vdots \\ R_{d,2k} & \ddots & R_{d,k} & \ddots & R_{d,0} \end{bmatrix} \tag{21}$$

is referred to as the *extended impedance* of the diode under specific voltage $v(t)$. The extended impedance matrix describes the constitutive coupling relation among different harmonics. Therefore, it can be used for the multiple harmonics analysis. Since the relation is a function of component state, say the voltage across a diode, iterative calculations are necessary for solving the numerical impedance matrix under steady-state operation.

REFERENCES

[1] Balato, M., Costanzo, L., and Vitelli, M., "Mppt in wireless sensor nodes supply systems based on electromagnetic vibration harvesters for freight wagons applications," *IEEE Transactions on Industrial Electronics* **64**(5), 3576–3586 (2017).

[2] Wang, S.-W., Ke, Y.-W., Huang, P.-C., and Hsieh, P.-H., "Electromagnetic energy harvester interface design for wearable applications," *IEEE Transactions on Circuits and Systems II: Express Briefs* **65**(5), 667–671 (2018).

[3] Cho, J. Y., Choi, J. Y., Jeong, S. W., Ahn, J. H., Hwang, W. S., Yoo, H. H., and Sung, T. H., "Design of hydro electromagnetic and piezoelectric energy harvesters for a smart water meter system," *Sensors and Actuators A: Physical* **261**, 261–267 (2017).

[4] Torah, R., Glynne-Jones, P., Tudor, M., O'donnell, T., Roy, S., and Beeby, S., "Self-powered autonomous wireless sensor node using vibration energy harvesting," *Measurement science and technology* **19**(12), 125202 (2008).

[5] Cheng, S., Wang, N., and Arnold, D. P., "Modeling of magnetic vibrational energy harvesters using equivalent circuit representations," *Journal of Micromechanics and Microengineering* **17**, 2328–2335 (oct 2007).

[6] Zhou, S., Jean-Mistral, C., and Chesné, S., "Influence of internal electrical losses on optimization of electromagnetic energy harvesting," *Smart Materials and Structures* **27**, 085015 (jul 2018).

[7] Liang, J., Ge, C., and Shu, Y.-C., "Impedance modeling of electromagnetic energy harvesting system using full-wave bridge rectifier," *Proc.SPIE* **10164**, 10164 – 10164 – 10 (2017).

[8] Liang, J. and Liao, W.-H., "Simulation and optimization of class-e power amplifiers with extended impedance method," in [*IEEE International Symposium on Circuits and Systems (ISCAS 2019)*], 2493–2496, IEEE (2009).

[9] Liang, J. and Liao, W.-H., "Steady-state simulation and optimization of class-e power amplifiers with extended impedance method," *IEEE Transactions on Circuits and Systems I: Regular Papers* **58**(6), 1433–1445 (2011).

[10] Liang, J., "Design of class-e power amplifier with nonlinear components by using extended impedance method," in [*IEEE International Symposium on Circuits and Systems (ISCAS 2016)*], 437–440, IEEE (2016).